

Interface effects and the evolution of ferromagnetism in $\text{La}_{2/3}\text{Sr}_{1/3}\text{MnO}_3$ ultrathin films

M Veis¹, M Zahradnik¹, R Antos¹, S Visnovsky¹, Ph Lecoeur², D Esteve², S Autier-Laurent², J-P Renard² and P Beauvillain²

¹ Charles University in Prague, Faculty of Mathematics and Physics, Ke Karlovu 3, 12116 Prague 2, Czech Republic

² Institut d'Electronique Fondamentale, IEF/UMR 862, Université Paris Sud XI, F-91405 Orsay Cedex, France

E-mail: veis@karlov.mff.cuni.cz

Received 6 September 2013

Accepted for publication 30 October 2013

Published 3 December 2013

Abstract

Pulse laser deposited $\text{La}_{2/3}\text{Sr}_{1/3}\text{MnO}_3$ ultrathin films on SrTiO_3 substrates were characterized by polar and longitudinal Kerr magneto-optical spectroscopy. Experimental data were confronted with theoretical simulations based on the transfer matrix formalism. An excellent agreement was achieved for a 10.7 nm thick film, while a distinction in the Kerr effect amplitudes was obtained for a 5 nm thick film. This demonstrated the suppression of ferromagnetism due to the layer/substrate interface effects. A revised, depth-sensitive theoretical model with monolayer resolution described the experimental data well, and provided clear cross-section information about the evolution of ferromagnetism inside the film. It was found that the full restoration of the double-exchange mechanism, responsible for the ferromagnetic ordering in $\text{La}_{2/3}\text{Sr}_{1/3}\text{MnO}_3$, occurs within the first nine monolayers of the film. Moreover, all the studied films exhibited magneto-optical properties similar to bulk crystals and thick films. This confirmed a fully developed perovskite structure down to 5 nm.

Keywords: magneto-optics, manganites, magneto-optical Kerr effect, ultrathin films, interface effects

1. Introduction

Hole-doped manganites $\text{La}_{1-x}\text{M}_x\text{MnO}_3$ ($M = \text{Ca}, \text{Sr}, \text{Ba}$) with perovskite-type structure have been intensively studied in the last decades due to their unique physical properties. The colossal magnetoresistance effect [1] and extremely high degree of spin polarization make them promising candidates for applications in spintronics. Their structural, magnetic and electric properties are strongly correlated, and can be optimized by proper choice of substrate, doping level and deposition conditions. It was realized that the large number of degrees of freedom in manganites could be used to design their physical properties according to some specific

function. This large variety and tunability of the physical properties (ferromagnetism, antiferromagnetism, metallicity, superconductivity, optical properties, etc) provides notable advantages for application to various devices. New devices, such as all-oxide spin field-effect transistors [2], magnetic tunnel junctions [3] and multiferroic memories [4], often include mixed-valence manganites as metallic contacts with well-defined magnetic ordering.

Many investigations have been focused on $\text{La}_{2/3}\text{Sr}_{1/3}\text{MnO}_3$ (LSMO), which shows the highest Curie temperature among the family of manganites ($T_C \sim 370$ K) [5]. Furthermore, it exhibits almost 100% spin polarization [6] and the largest single electron bandwidth, which is very important from the point of view of application. Ferromagnetic properties of LSMO are dominated by the double-exchange (DE) interaction, which originates from the e_g electron transfer between Mn^{3+} and Mn^{4+} ions via



Content from this work may be used under the terms of the Creative Commons Attribution-NonCommercial-ShareAlike 3.0 licence. Any further distribution of this work must maintain attribution to the author(s) and the title of the work, journal citation and DOI.

the O^{2-} 2p state. Since the DE electron transfer probability strongly depends on $Mn^{3+}-O-Mn^{4+}$ geometry (Mn–O bond lengths and/or $Mn^{3+}-O-Mn^{4+}$ bond angles), the main factors responsible for changes in magnetic properties are distortions of MnO_6 octahedra, mainly induced by the strain arising in the film from the lattice mismatched substrate [7]. When grown on $SrTiO_3$ (STO) substrates ($a = 0.3905$ nm, cubic) a tensile strain is induced in the LSMO layer, resulting in an elongation of, a , the in-plane lattice parameter with respect to the bulk value ($a_{LSMO\text{ bulk}} = 0.3889$ nm) and compression of, c , the out-of-plane lattice parameter. The variation of the c/a ratio as a function of thickness was reported to be negligible [8], reflecting a fully strained state without any relaxation parameter between the interface and the surface up to 60 nm. It was shown that the three-dimensional compression and biaxial distortions affect T_C [7, 9].

Physical properties considerably different from bulk crystals were observed in LSMO ultrathin films (with thickness below 10 nm) [10, 11]. The origin of such an effect, attributed to the LSMO/STO interface, was recently extensively discussed in literature [12–17]. However, owing to the complex structure of LSMO, a confusing variety of physical mechanisms has been proposed, including a homogeneous strain [18] and phase separation phenomena [19–21] related to the presence of structural inhomogeneities localized at the interface between the film and the substrate [22].

Recently, Tebano *et al* [13, 14] reported that the origin of the interface effects is related to the suppression of the DE mechanism due to the broken symmetry at the interfaces. This stabilizes the out-of-plane Mn e_g ($3z^2 - r^2$) orbitals against in-plane e_g ($x^2 - y^2$) making a local C-type antiferromagnetic structure at the interface [13]. On the other hand, a fingerprint of the ($x^2 - y^2$) preferential orbital ordering was observed by linear dichroism of the x-ray absorption (LD-XAS) in films with the thickness 20 nm (50 monolayers (ML)). Such orbital character was even more visible in relatively thick (100 ML, roughly 40 nm), fully strained LSMO/STO films ($c/a = 0.98$). These films displayed metallic ferromagnetic properties with $T_C \sim 370$ K, identical to the bulk value [13] and magneto-optical properties of such thick films ($t \geq 35$ nm) are comparable with those of bulk crystals [23, 24]. In sharp contrast, Huijben *et al* [15] observed by LD-XAS that the preferred orbital ordering remains ($x^2 - y^2$) for film thicknesses down to only a few MLs. Lepetit *et al* [12] proposed a simple model dealing with gradual restoration of DE interaction ML by ML. However, a clear experimental evidence of the evolution of ferromagnetism inside LSMO ultrathin films is still missing, since all the current experiments have been done on sets of samples with various thicknesses and without the depth sensitivity.

Magneto-optical spectroscopy offers an opportunity to study the physical properties of magnetic materials when other conventional methods might not be effective. It can be used as a depth-sensitive technique to probe the magnetic properties throughout the studied system, giving a unique chance to study the evolution of the magnetism in the vicinity

of the LSMO/STO interface. Previous magneto-optical studies were focused on LSMO thin films (with thickness from 20 to 40 nm) [23, 24], thick films (with thickness from 50 to 300 nm) [25–28], crystalline pellets [29] and bulk crystals [30]. Since the magneto-optical Kerr effect is proportional to the magnetization M in the film, ultrathin films exhibit extremely small angles of the Kerr rotation and ellipticity, requiring a high sensitivity experimental magneto-optical setup. Therefore a systematic study of the magneto-optical properties of LSMO films with thicknesses below 10 nm is still missing.

Here, we report the magneto-optical properties of LSMO ultrathin films grown by pulsed laser deposition (PLD) on single crystal (100) STO substrates. With the help of theoretical models, we provide clear evidence of the evolution of magnetism in the vicinity of the LSMO/STO interface.

2. Experimental methods

Studied films were grown by PLD from a stoichiometric target under low oxygen pressure of 120 mTorr using a KrF laser at a wavelength of 248 nm. The maximum energy fluence was 3 J m^{-2} with a pulse repetition rate of 1 Hz and the substrate was heated to 893 K during the deposition. These parameters were found to be optimal for single-crystalline film growth. Low pressure PLD under a strong oxidizing gas allows ‘cell-by-cell’ growth which can be monitored *in situ* using reflective high-energy electron diffraction and which produces high quality epitaxial films or superlattices [7]. The quality of interfaces along with smoothness of the surface was further increased by modification of the laser beam using a spatial filter, which acted as a beam homogenizer. The surface roughness was probed by atomic force microscopy and was found to be lower than 0.2 nm for all investigated films. The thickness, t , of LSMO layers was measured by x-ray diffraction (XRD) and x-ray reflectivity as 5 nm (13 ML) and 10.7 nm (27 ML). The out-of-plane parameter, c , of LSMO layers was obtained from XRD patterns using (002) LSMO peak. The values are $c = 0.3845$ nm for the 10.7 nm-thick sample and $c = 0.3833$ nm for the 5 nm thick sample, indicating fully strained LSMO layers. Magnetometry measurements proved T_C above room temperature for both samples.

The magneto-optical spectroscopy was carried out in the polar and longitudinal configuration using an azimuth modulation technique with synchronic detection³. The experiment was carried out in the photon energy range between 1.2 and 4.6 eV. The experimental optical setup included a 450 W Xe arc lamp, quartz prism monochromator, polarizer, dc compensating Faraday rotator, ac modulating Faraday rotator, phase plate (for Kerr ellipticity measurements), the sample in magnetic field, analyzer and photomultiplier. In the small angle approximation the complex polar magneto-optical Kerr effect was measured at nearly normal light incidence as a ratio $\theta_K + i\varepsilon_K \approx (r_{yx}/r_{xx})$ of Jones reflection matrix elements, where θ_K and ε_K are the

³ The magneto-optical spectrometer operating at the Institute of Physics of Charles University in Prague since 1975 was built by one of us (SV).

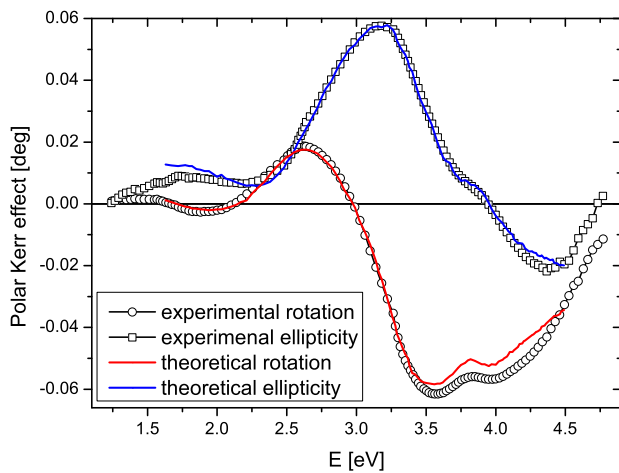


Figure 1. Experimental and theoretical polar Kerr rotation and ellipticity spectra of 10.7 nm thick LSMO film. The experimental spectra were obtained for nearly normal light incidence. The theoretical model employed transfer matrix formalism and bulk-like material parameters of a 35 nm thick LSMO layer.

Kerr rotation and ellipticity. The longitudinal magneto-optical Kerr effect was measured similarly at the angle of incidence adjusted to 56° for p -polarized incident light as a ratio $\theta_K + i\varepsilon_K \approx (r_{ps}/r_{pp})$ [23]. The applied magnetic field was 470 and 100 mT in the polar and longitudinal configuration, respectively. In both configurations the magnetic field was sufficient for the film saturation (as was checked by the measurement of magnetic field dependence of the magneto-optical Kerr effect). During the polar configuration measurements the samples were placed on a water-cooled pole piece of electromagnet and their temperature was stabilized at 285 K. In the longitudinal configuration measurements the samples were kept at the stabilized room temperature of 295 K.

Theoretical calculations were performed using the transfer matrix approach [31] and assuming film uniformity. Since the unpolished, back side of the STO substrate was depolarizing and therefore had a negligible contribution to optical reflection, we focused ourselves on a model of a single- or multi-layer on a semi-infinite substrate. For strained LSMO layers this model (assuming a flat surface and planar interface between the LSMO layer and STO substrate) represents a reasonable approximation.

3. Results and discussion

Figure 1 displays experimental polar Kerr rotation and ellipticity spectra for the sample with the thickness $t = 10.7$ nm. Two opposite spectroscopic peaks (centered near 2.7 and 3.6 eV) dominate the Kerr rotation spectrum and one positive peak (centered near 3.4 eV) dominates the Kerr ellipticity spectrum. Two electronic transitions are responsible for such spectroscopic structures in polar Kerr spectra. Both transitions involve Mn 3d orbitals and can be assigned to a dipole-forbidden spin-allowed intra-3d-Mn crystal field transition (centered near 2.7 eV) and charge-transfer transition

O 2p \rightarrow Mn 3d e_g (centered near 3.6 eV). Such assignment was recently confirmed by *ab initio* calculations [25, 27].

The spectra in figure 1 exhibit similar spectral behavior to previously published magneto-optical studies on thin films [23, 24], thick films [25], crystalline pellets [29] and bulk crystals [30]. A splitting of the negative peak in the Kerr rotation spectrum is clearly visible near 3.7 eV. This effect was observed only for layers with thicknesses below 20 nm [23, 24]. It originates from the STO substrate, as was found by spectroscopic ellipsometry measurements on bare STO crystals, and can be seen due to a reduced penetration depth, which is approximately 30 nm at this photon energy. The smoothness of the experimental spectra (with low level of noise) demonstrates the high optical quality of the surface. The obtained spectra exhibit higher amplitudes than previously published results on LSMO films with similar thicknesses [23, 24]. This points to the higher magnetization of the investigated film, which was achieved by a homogenized laser beam.

Model spectra of a single LSMO layer on STO substrate are included in figure 1. Bulk-like optical and magneto-optical constants (diagonal and off-diagonal elements of permittivity tensor ε_{xx} and ε_{xy}) obtained on a 35 nm thick LSMO layer on STO (100) substrate [23] were adopted in this calculation. Optical constants of STO substrate (diagonal elements of permittivity tensor ε_{xx}) used in the calculation were acquired from spectroscopic ellipsometry measurements on bare STO substrates [24]. An excellent agreement between experimental data and theoretical calculations is clearly visible. A small deviation in the UV region can be explained by slightly better functionality of the current magneto-optical setup, which employs a photomultiplier detector with enhanced UV sensitivity. The broadening of the Kerr rotation at 3.7 eV is also well reproduced, because the layer thickness and the back reflections from the layer/substrate interface are both considered in the calculation procedure. The agreement between the theoretical and experimental spectra indicates the well-defined and flat STO/LSMO interface, because the model structure considers planar interfaces without any change of magnetic properties throughout the layer. It appears that interfacial effects between the LSMO layer and STO substrate, which are the reason for magnetization lost at the interface, has an insignificant influence on the magneto-optical properties in the investigated film (i.e. they occur at a short distance in the proximity of the interface). Since the material parameters of the 35 nm thick layer provided an excellent agreement between the experiment and theoretical calculation, it is evident that the magneto-optical properties of a 10.7 nm thick film are close to those of bulk crystals.

Figure 2 shows the experimental polar Kerr rotation and ellipticity spectra for 5 nm thick film. The experimental data show spectroscopic features typical for LSMO single-crystalline layers, giving a clear evidence of a fully developed LSMO structure with ferromagnetic behavior at room temperature. This is a clear improvement with respect to previous reports [12, 13], where T_C was evaluated lower than 280 K. Moreover, the low level of noise in the

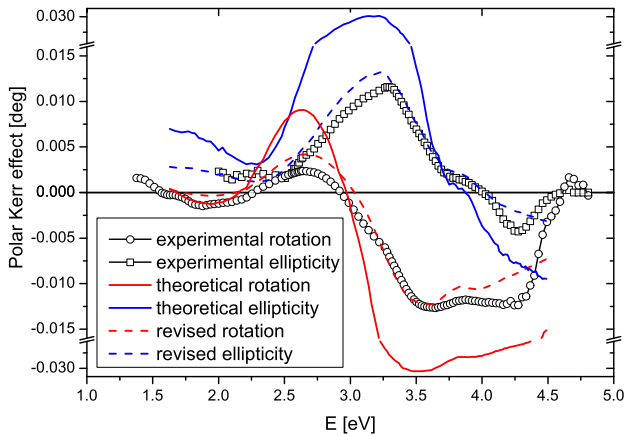


Figure 2. Experimental and theoretical polar Kerr rotation and ellipticity spectra of 5 nm thick LSMO film. The experimental spectra were obtained for nearly normal light incidence. The theoretical model (solid curves) employed transfer matrix formalism and material parameters of a 35 nm thick LSMO layer. The revised theoretical model (dashed curves) considered a more realistic structure displayed in figure 3(a).

spectra reflects a high optical quality of the surface. Since the experimental data in figure 2 do not show any significant spectral broadening of the magneto-optical transition lines, the O 2p band stays strongly hybridized with the Mn 3d band although the film thickness is reduced.

Theoretical polar Kerr spectra were calculated using the same material parameters as for the thicker sample, and are included (as solid curves) in figure 2. With respect to previously published results [12, 13, 15], which showed suppressed ferromagnetism in LSMO layers below 18 ML (~ 7 nm) in thickness, we should observe a difference between theoretical and experimental polar Kerr spectra. Indeed, although the theoretical spectral dependence follows the experimental data reasonably, there is a notable difference in their amplitudes. This is a clear evidence of the influence of LSMO/STO interface effects on magneto-optical properties in LSMO ultrathin films.

Lepetit *et al* [12] suggested a simple model of the LSMO/STO interface effects adopting the orbital reconstruction mechanism proposed by Tebano *et al* [13]. In this model, the preferred ($3z^2 - r^2$) ordering is located only in the proximity of the interface (in the thickness of 3 ML) and completely suppresses the DE interactions. In following layers, the ($3z^2 - r^2$) occupations start to relax toward more balanced ($x^2 - y^2$) orbitals. This is followed by the enhancement of T_C . After approximately 8 ML, T_C is saturated and the DE is fully restored, resulting in ferromagnetic properties and high T_C in films thicker than 14 ML [12]. Adopting this model, a more realistic model structure for theoretical calculation was considered. This structure consists of: STO substrate; a 6 ML thick layer, optically matched with LSMO but without DE interactions and ferromagnetic ordering; a 3 ML thick layer, optically matched with LSMO and increasing DE with each ML; a 4 ML thick bulk LSMO. A proper intensity of the DE interactions and thus ferromagnetic properties was selected by the modification of the off-diagonal permittivity elements of LSMO. A schematic picture of the

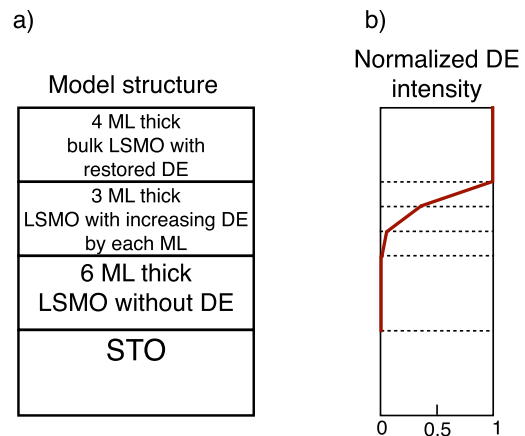


Figure 3. (a) A realistic model structure used in magneto-optical simulations of a 5 nm thick LSMO layer consisting of 13 ML. (b) Obtained cross-section scheme of the evolution of DE interactions throughout the layer.

model structure is displayed in figure 3(a). Corresponding theoretical spectra are included (as dashed curves) in figure 2.

A very good agreement between experimental data and revised theoretical spectra is clearly visible in figure 2. The spectral dependence of the experimental data is well reproduced by the theoretical calculation and the deviations are within the errors of both, the experimental data and the material parameters. Since the model still considers sharp and flat interfaces of homogeneous magnetic layers, the DE suppression by the phase separation on the LSMO/STO interface is ruled out in our case.

The model provided valuable cross-section information about the DE evolution inside the film, which is shown in figure 3(b). The dominating ($3z^2 - r^2$) ordering is associated with the first three ML of the film, completely smearing the in-plane DE. We believe that in the next three MLs the Mn e_g occupations start to relax, however the intensity of DE is still too small to provide a ferromagnetic contribution of these layers at room temperature. Low temperature measurements would be necessary to provide detailed information about magneto-optical properties in these layers.

After approximately 6 ML, increasing in-plane ($x^2 - y^2$) occupation raises the DE mechanism, resulting in a clearly visible magneto-optical contribution of subsequent layers. As follows from figure 3(b), the increase of DE intensity is quite fast. Therefore, within the first nine MLs the Mn e_g orbital occupation is relaxed from the interfacial ($3z^2 - r^2$) to the preferred ($x^2 - y^2$), resulting in the full restoration of the DE mechanism.

Experimental Kerr rotation and ellipticity spectra measured in longitudinal configuration together with theoretical models for a 10.7 nm thick LSMO layer are shown in figure 4. The spectra are similar in shape to previously published results [23]. The theoretical model describes the experimental spectra reasonably and the deviations can be assigned to the higher temperature during longitudinal measurements (approximately 10 K higher), since the ferromagnetic properties of LSMO are strongly temperature dependent near T_C . Therefore the higher temperature of the

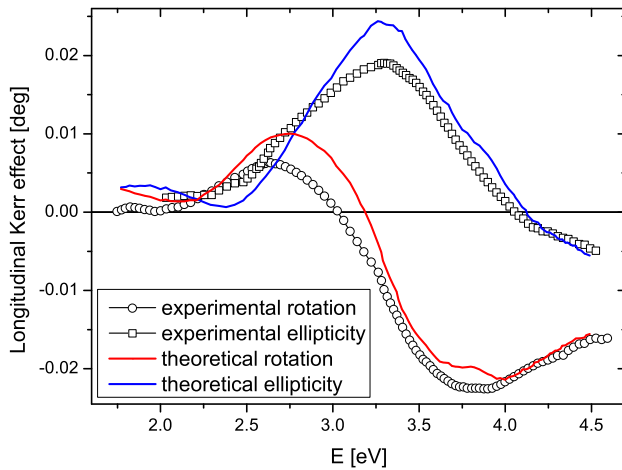


Figure 4. Experimental and theoretical longitudinal Kerr rotation and ellipticity spectra of 10.7 nm thick LSMO film. The angle of light incidence was adjusted to 56° . The incident light was p -polarized. The theoretical spectra were calculated similarly to the polar case.

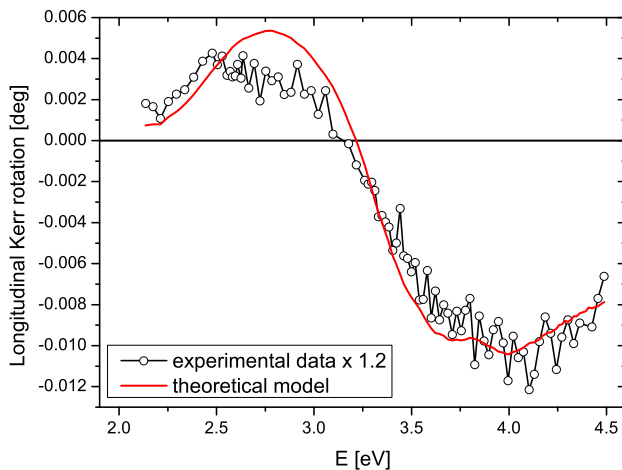


Figure 5. Experimental (symbols) and theoretical (solid curve) longitudinal Kerr rotation spectra of 5 nm thick LSMO film. The angle of light incidence was adjusted to 56° . The incident light was p -polarized. The theoretical spectrum was calculated similarly to the polar case, considering the model structure displayed in figure 3(a).

sample results in smaller amplitudes of the magneto-optical effect.

Experimental and theoretical longitudinal Kerr rotation spectra of a 5 nm thick LSMO layer are displayed in figure 5. Despite a higher level of noise, the spectral dependence of the longitudinal Kerr rotation is noticeably similar to that of the thicker sample. The higher level of noise is due to a very small Kerr effect amplitude, which is of the order of millidegrees. Such a value is at the edge of the experimental system's sensitivity. The theoretical spectral dependence of longitudinal Kerr rotation describes the experimental spectrum well. This confirms a proper choice of the multilayer model structure with different intensities of DE in each ML. Notable differences in amplitudes can be attributed to the higher measurement temperature (here the temperature dependence of the Kerr effect amplitude is much stronger

with respect to the very small sample thickness) as well as to the measurement error of the magneto-optical setup for such small Kerr angles. However, the visible longitudinal spectrum of a 5 nm thick LSMO layer is a good demonstration of the magneto-optical setup efficiency in the probing of magnetic properties down to the nanometer scale.

4. Conclusions

In conclusion, we have reported the magneto-optical properties of ultrathin LSMO films grown on STO substrates. All films displayed spectral properties of the magneto-optical Kerr effect similar to those of bulk crystals. Bulk-like magneto-optical properties of 10.7 nm thick film were confirmed by excellent agreement between experimental data and theoretical calculations. A realistic model, including the change of ferromagnetism inside the film was employed to correctly describe the experimental Kerr magneto-optical spectra of a 5 nm thick sample. This model with ML resolution provided clear information about the evolution of the DE mechanism inside the LSMO layer. It was found that the DE is fully restored within the first nine MLs on the substrate. Furthermore, the visible spectrum of the longitudinal Kerr rotation of 5 nm thick film clearly demonstrated that magneto-optical spectroscopy is a highly effective and depth-sensitive experimental method to probe the physical properties of magnetic nanostructures.

Acknowledgment

This work was supported by the Czech Science Foundation grant no. P204/10/P346.

References

- [1] von Helmolt R, Wecker J, Holzapfel B, Schultz L and Samwer K 1993 *Phys. Rev. Lett.* **71** 2331
- [2] Ahn C H, Triscone J M and Mannhart J 2003 *Nature* **424** 1015
- [3] Alldredge L M B, Chopdekar R V, Nelson-Cheeseman B B and Suzuki Y 2006 *Appl. Phys. Lett.* **89** 182504
- [4] Gajek M, Bibes M, Fusil S, Bouzêhouane K, Fontcuberta J, Barthelemy A and Fert A 2007 *Nature Mater.* **6** 296
- [5] Jonker G H and Van Santen J H 1950 *Physica* **16** 337
- [6] Bowen M, Bibes M, Barthelemy A, Contour J P, Anane A, Lemaître Y and Fert A 2003 *Appl. Phys. Lett.* **82** 233
- [7] Haghiri-Gosnet A M and Renard J P 2003 *J. Phys. D: Appl. Phys.* **36** R127
- [8] Haghiri-Gosnet A M, Wolfman J, Mercey B, Simon Ch, Lecoer P, Korzenski M, Hervieu M, Desfeux R and Baldinozzi G 2000 *J. Appl. Phys.* **88** 4257
- [9] Millis A J, Darling T and Migliori A 1998 *J. Appl. Phys.* **83** 1588
- [10] Sun J Z, Abraham D W, Rao R A and Eom C B 1999 *Appl. Phys. Lett.* **74** 3017
- [11] Wang J, Hu F X, Li R W, Sun J R and Shen B G 2010 *Appl. Phys. Lett.* **96** 052501
- [12] Lepetit M B, Mercey B and Simon Ch 2012 *Phys. Rev. Lett.* **108** 087202
- [13] Tebano A et al 2008 *Phys. Rev. Lett.* **100** 137401
- [14] Tebano A et al 2010 *Phys. Rev. B* **82** 214407

- [15] Huijben M, Martin L W, Chu Y H, Holcomb M B, Yu P, Rijnders G, Blank D H A and Ramesh R 2008 *Phys. Rev. B* **78** 094413
- [16] Lee J S, Arena D A, Yu P, Nelson C S, Fan R, Kinane C J, Langridge S, Rossell M D, Ramesh R and Kao C C 2010 *Phys. Rev. Lett.* **105** 257204
- [17] Herger R et al 2008 *Phys. Rev. B* **77** 085401
- [18] Ziese M, Semmelhack H C and Han K H 2003 *Phys. Rev. B* **68** 134444
- [19] Becker T, Streng C, Luo Y, Moshnyaga V, Damaschke B, Shannon N and Samwer K 2002 *Phys. Rev. Lett.* **89** 237203
- [20] Dagotto E, Hotta T and Moreo A 2001 *Phys. Rep.* **344** 1
- [21] Biswas A, Rajeswari M, Srivastava R C, Venkatesan T, Greene R L, Lu Q, de Lozanne A L and Millis A J 2001 *Phys. Rev. B* **63** 184424
- [22] Bibes M, Balcells L, Valencia S, Fontcuberta J, Wojcik M, Jedryka E and Nadolski S 2001 *Phys. Rev. Lett.* **87** 067210
- [23] Veis M, Visnovsky S, Lecoeur Ph, Haghiri-Gosnet A M, Renard J P, Beauvillain P, Prellier W, Mercey B, Mistrik J and Yamaguchi T 2009 *J. Phys. D: Appl. Phys.* **42** 195002
- [24] Mistrik J et al 2006 *J. Appl. Phys.* **99** 08Q317
- [25] Liu H L, Lu K S, Kuo M X, Uba L, Uba S, Wang L M and Jeng H T 2006 *J. Appl. Phys.* **99** 043908
- [26] Liu H L, Zhang Y J, Wu L C, Uba L, Uba S, Chang W J, Lin J Y and Wang L M 2006 *J. Magn. Magn. Mater.* **304** e303
- [27] Uba L, Uba S, Germash L P, Bekenov L V and Antonov V N 2012 *Phys. Rev. B* **85** 125124
- [28] Fumagalli P, Spaeth Ch and Guntherodt G 1995 *IEEE Trans. Magn.* **31** 3277
- [29] Popma T J A and Kamminga M G J 1975 *Solid State Commun.* **17** 1073
- [30] Rauer R, Neuber G, Kunze J J, Bäckström Rübhausen M, Walter T and Dörr K 2005 *J. Magn. Magn. Mater.* **290** 948
- [31] Yeh P 1980 *Surf. Sci.* **96** 41